24. ANTHROPOGENIC INFLUENCE ON THE EASTERN CHINA 2016 SUPER COLD SURGE

Ying Sun, Ting Hu, Xuebin Zhang, Hui Wan, Peter Stott, and Chunhui Lu

Human influence decreased the probability of a cold surge occurrence in China.

Introduction. A super cold surge during the winter of December 2015 to February 2016 was widely reported by Chinese media. This cold surge originated from the Siberian High and swept across the country on 21–25 January 2016, bringing very strong winds and a large and sudden fall in temperature. During the cold surge, air temperatures dropped more than 12°C over 18% of the country and by 6°C over more than 80% of the country. More than 95% of the country experienced frigid winter weather with minimum temperatures below 0°C (Jiang et al. 2016). Record-breaking minimum temperatures were reported at many observing stations, with temperature at −46.8°C observed in the Inner Mongolia autonomous region. The lives of more than one billion people were affected by this cold surge. Snowfall occurred in Guangzhou, the capital city in one of the southernmost provinces in China—the first ever snow event since the meteorological observing station was established. Extreme weather brought by the cold surge, such as heavy snowfall, freezing rain, and frost, caused significant impacts on transportation and electricity transmission systems, and on agriculture and human health (CMA 2017).

One would naturally expect a reduction in cold extremes as a result of global warming. Nevertheless, some studies have suggested that Arctic amplification of warming and Arctic sea ice loss may have contributed to the so-called "warm Arctic–cold Eurasia" pattern over the past few decades (e.g., Cohen et al. 2014; Mori et al. 2014). It has therefore been speculated that continued Arctic sea ice loss would cause more cold extremes in the continental midlatitudes. This does not seem to be the case in the United States where very cold winters have become less likely due to global warming (Wolter et al. 2015; Trenary et al. 2016). In China, a few recent studies have shown that the decrease in the intensity and frequency of cold extremes can be attributed to human influence (Yin et al. 2016; Lu et al. 2016) although the attribution of cold surge events has not yet been resolved. Here we examine a related question with regard to long-term change in extreme cold surges, such as the 2015 winter cold surge in eastern China, and possible causes of the change.

Data and methods. We use the gridded daily minimum temperature available from the China National Meteorological Information Center. The data is on a 0.5° × 0.5° grid and is based on the homogenized daily temperatures at 2419 stations (Cao et al. 2016). These data were converted to 2° × 2° resolution prior to subsequent analyses. As the cold surge mainly affected the eastern part of China that is within the East Asian monsoon region, we focus on three large north–south regions, including Northern China (NC; 36°–46°N, 104°–124°E), the lower Yangtze River Valley (YRV; 28°–36°N, 104°–124°E) and Southern China (SC; 18°–28°N, 104°–124°E). These regions are marked by the red boxes in Fig. 24.1a. We use the lowest regional average of daily minimum 2-m temperatures (TNn) in winter months (December–February) to represent the severity of a large-scale cold air outbreak. The regional averages were obtained by area weighting the gridded data available within each region. Regional anomalies of TNn relative to 1961–90 average are retained for the subsequent analyses.

Daily minimum temperatures simulated by the climate models participating in the Coupled Model Intercomparison Project Phase 5 (CMIP5) are also used. This includes 62 simulations from 16 models forced with the combined effect of anthropogenic and natural external forcings (ALL) and 26 simulations from 6 models forced with the natural external

AFFILIATIONS: Sun—National Climate Center, China Meteorological Administration, Beijing, and Collaborative Innovation Center on Forecast and Evaluation of Meteorological Disasters, Nanjing University of Information Science & Technology, Nanjing, China; Hu and Lu—National Climate Center, China Meteorological Administration, Beijing, China; Zhang and Wan—Climate Research Division, Environment and Climate Change Canada, Toronto, Ontario, Canada; Stott—Met Office Hadley Centre, Exeter, United Kingdom

DOI:10.1175/BAMS-D-17-0092.1

A supplement to this article is available online (10.1175/BAMS-D-17-0092.2)

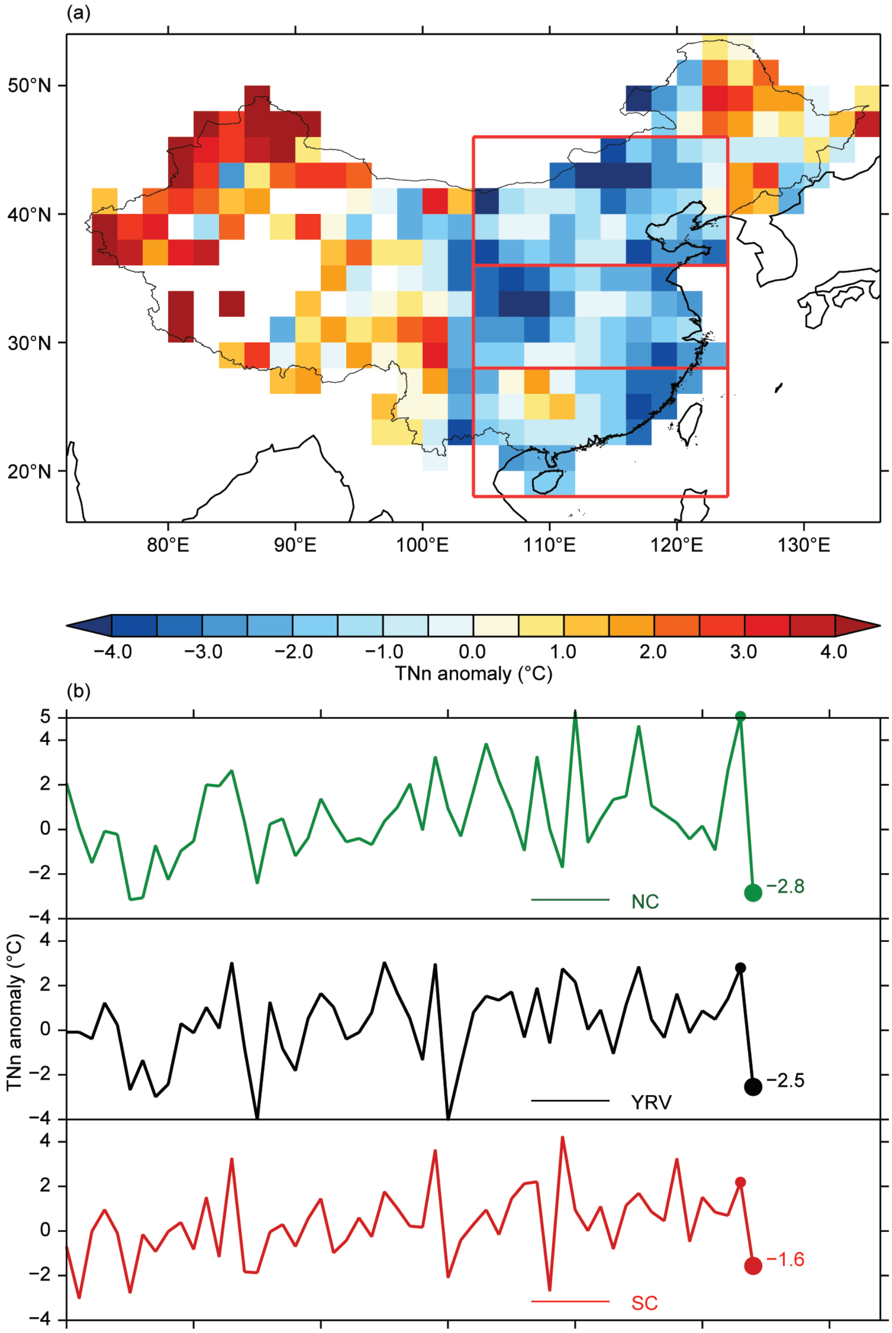

Fig. 24.1. (a) 2015/16 winter TNn anomalies (°C). Boxes indicate NC, YRV, and SC regions; see text for coordinates. (b) Time series of winter regional mean TNn anomalies (°C) in NC (green), YRV (black), and SC (red). The numbers indicate anomalies for 2015/16 winter.

forcings only (NAT). These simulations are used to estimate the model response to ALL and NAT forcings respectively. Pre-industrial control simulations from 28 models are also used in the estimation of natural variability. Details about the simulations and procedures for processing the model data are given in Table ES24.1 and the other online supplement material.

Our method is similar to Sun et al. (2014); it involves the detection and attribution analysis and estimate of relative risk of an event in the world with or without human influence. For the detection and attribution analysis, we consider spatial averages of daily minimum temperature over a large region which has a strong temporal persistence. Because of this, the minimum values sampled from area average daily minimum temperature over a winter have a symmetric probability distribution rather than an extreme value distribution. We therefore apply the total least square (TLS) method (Allen and Stott 2003) to regress the observations onto ALL and NAT signals computed as multimodel ensemble means of the relevant simulations. The regression is conducted on space–time series of 3-winter non-overlapping mean series for winters 1961/62 through 2011/12 over the three spatial domains. The use of a 3-winter mean series is a compromise for reducing temporal dimension as well as variability but still retaining climate response to volcanic forcing. The covariance matrix required for solving the regression problem is based on regularized co-variance matrix described in Ribes et al. (2013) as this estimator is more robust. The regression coefficient is called the scaling factor, indicating the magnitude that simulated signal must be scaled to best match the observations. A signal is detected if the 90% confidence interval (CI) of the corresponding scaling factor is above zero. To estimate relative risk, we first multiply the ALL and the NAT signals by the corresponding scaling factors to obtain the observation-constrained best estimates of ALL and NAT response in winters 2013/14–2015/16. We use ensemble mean of RCP4.5 simulation to represent ALL signal in winters 2013/14–2015/16 (red dots in Figs. 24.2a–c). The NAT experiments end in 2012, so we simply use the NAT signal for winters 2009/10–2011/12 for winters 2013/14–2015/16 (blue dots in Figs. 24.2a–c). This is justified since there was no major difference in the levels of volcanic activity between the two three-year periods. The scaling factors are obtained from the two-signal detection analysis in which observations are regressed simultaneously to ALL and NAT signals. We then add the preindustrial control simulations to these best estimates to reconstruct extreme temperature series representative of the 2015/16 winter climate in the world with or without human influence. The probabilities of a cold surge of the magnitude of the 2015/16 winter event in the world with *(p1)* or without *(p0)* anthropogenic influence are the percentages of times when temperature anomalies are at or below the observed 2015/16 winter value in the relevant series. The relative risk or risk ratio (RR) is defined as RR = $p1/p0$. The CI of the risk ratio was estimated from 1000 random samples of scaling factors assuming the scaling factors follow normal distributions.

Results. Figure 24.1a shows the TNn anomalies in the 2015/16 winter. Negative anomalies were observed in most areas of eastern China (east of 105°E), with the largest anomalies below −3.5°C appearing in central and northern China. This strong negative anomaly is in sharp contrast with continuous warming in winter mean temperature in recent decades (MOST 2016). In fact, the 2015/16 winter mean temperature was slightly higher than the 1971–2000 average (CMA 2017). The coldest TNn for the 2015/16 winter occurred during this cold surge (21–25 January 2016) in most stations (not shown). The anomalies of winter minimum regional mean daily minimum temperature in the three regions NC, YRV, and SC (Fig. 24.1b) were −2.8°C, −2.5°C, and −1.6°C, respectively. They were ranked as the 3rd, 5th, and 7th coldest since 1961 for the respective regions.

Figures 24.2a–c show the observed and the simulated 3-winter mean non-overlapping series. The observed TNn has increased at the rates of 0.43°C decade^{-1}, 0.35°C decade^{-1}, and 0.41°C decade^{-1} for NC, YRV, and SC, respectively, during 1961/62 winter through 2011/12 winter. The linear trends (dashed lines) in the simulated responses to ALL forcing are 0.25°C decade^{-1}, 0.17°C decade^{-1}, 0.15°C decade^{-1}, respectively, indicating that the models may have underestimated the observed changes. The NAT trends are 0.10°C decade^{-1}, 0.11°C decade^{-1}, 0.07°C decade^{-1},

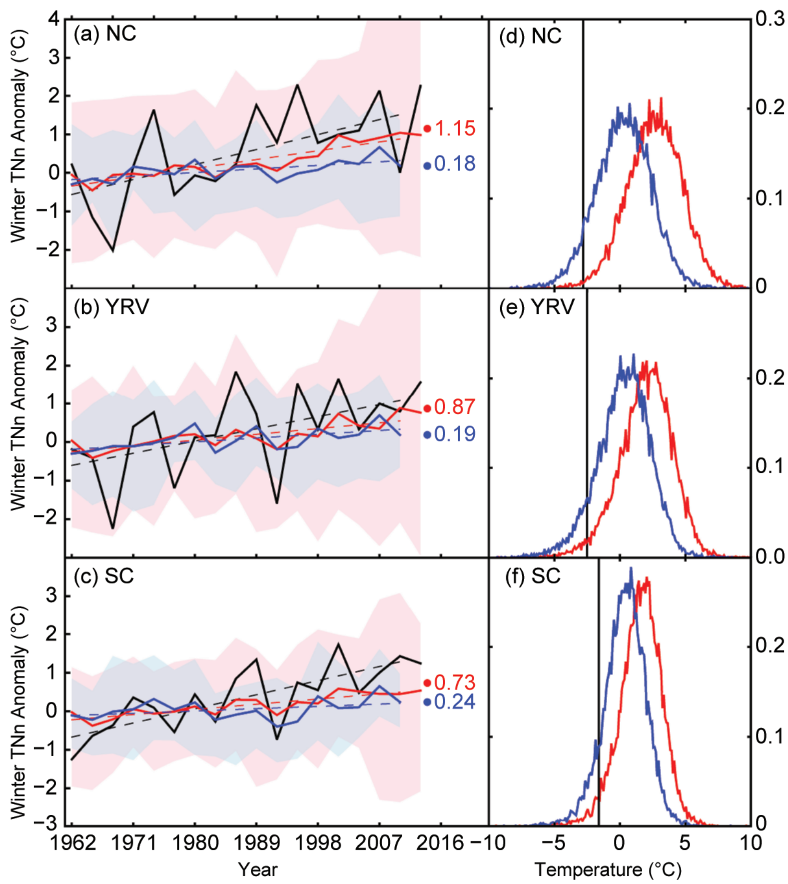

Fig. 24.2. The 3-year winter mean non-overlapping TNn anomalies (°C) from the observations (black) and model simulations under ALL (red) and NAT (blue) forcings for (a) NC, (b) YRV, and (c) SC regions. Red and blue lines indicate multimodel ensemble mean. Dashed lines show long term trends. Reconstructions of the 3-year winter mean for ALL forcings in winters 2013/14–2015/16 and NAT forcings in winters 2009/10–2011/12 are marked with red (ALL) and blue (NAT) dots and numbers. Pink and blue shadings show the 5%–95% ranges of the individual model simulations from ALL and NAT experiments, respectively. Histograms of the winter minimum regional mean TNn anomalies (°C) for (d) NC, (e) YRV, and (f) SC, under NAT (blue) ALL (red) forcing. The black lines indicate the 2015/16 winter anomalies.

respectively, suggesting a possibility for NAT forcing to contribute to the observed warming. Note however that models may have overestimated NAT response since CMIP5 underestimates volcanic aerosols for the 21st century (Santer et al. 2014). The scaling factors for anthropogenic forcing (ANT) and NAT are 2.45 (90% CI: 1.07–4.17) and 1.52 (90% CI: −0.68–3.47), respectively, in the two-signal detection analysis in which observed series is regressed to ALL and NAT simultaneously. This means that the observed changes in extreme winter temperature are mainly due to anthropogenic forcing. Natural external forcing may have contributed to observed trend but its contribution is not significantly different from zero. The observed TNn has a standard deviation of 1.91°C, 1.70°C, 1.54°C in NC, YRV, and SC, respectively. The best estimate of reconstructed series with both anthropogenic and natural forcings has a standard deviation of 2.28°C (90% CI: 1.64°–2.93°C), 2.16°C (90% CI: 1.47°–2.86°C), 1.74 °C (90% CI: 1.16°–2.31°C), respectively. The fact that the observed variability is slightly smaller but also generally comparable to that in the reconstructed series indicates that it is possible to produce a credible estimate of the probability of extreme temperature based on reconstructed series.

As shown in Figs. 24.2d–f, the empirical probability density of TNn shifts towards warmer temperatures in the world under anthropogenic influence in all three regions, meaning that anthropogenic influence decreased the probability of cold surge. Table 24.1 summarizes the results. External forcing may have warmed TNn by 2.6°C, 2.0°C, and 1.6°C in NC, YRV, and SC, respectively, by 2015. That is to say, the 2015/16 winter cold surge would have been much stronger without anthropogenic induced warming. The risk ratio for the event of 2015/16 winter magnitude is 0.11, 0.27, 0.31 for NC, YRV, and SC, respectively, meaning that the anthropogenic influence may have respectively reduced the occurrence of such a cold event by 89% (90% CI: 54%–98%) , 73% (90% CI: 37%–90%), and 69% (90% CI: 30%–86%).

Conclusions and discussion. The magnitude of winter cold surge has not increased in Eastern China. It has decreased due to anthropogenic influence. This is consistent with earlier findings of Yin et al. (2016) and Lu et al. (2016), who found that cold extremes in China have decreased due to anthropogenic influence. The recent super cold surge of Eastern China that occurred 21–25 January 2016 would have been much stronger if there was no human-induced warming. Alternatively, the occurrence for a cold surge with the magnitude of the 2015/16 winter event has been much reduced due to anthropogenic influence. Note that our quantification of anthropogenic influence on cold surge involves the comparison between ALL and NAT responses. As different sets of models are used in such a comparison, the results would also be impacted by this aspect of modeling uncertainty. Additionally, results can also be sensitive to the subsets of selected models because uncertainty in signal estimation becomes larger with a much-reduced number of simulations.

ACKNOWLEDGMENTS. We thank Martin Hoerling and two anonymous reviewers for their very helpful comments. Y.S. and T. H. are supported by China funding agencies through multiple grants: National Key R&D Program of China 2017YFA0603804, China NSFC 41675074, CCSF 201704, GYHY201406020. PAS was supported by the U.K.-China Research & Innovation Partnership

Table 24.1. Possible human influence on the cold surge like the 2016 January event.

TNn	NC	YRV	SC
Observed TNn anomaly	−2.8°C	−2.5°C	−1.6°C
Warming attributable to ALL forcing	2.6°C	2.0°C	1.6°C
Return period in a world without human influence	14 years (90% range 10–19 years)	12 years (90% range 9–15 years)	9 years (90% range 6–14 years)
Return period in a world with human influence	131 years (90% range 21–914 years)	42 years (90% range14–144 years)	28 years (90% range 8–97 years)
Risk ratio (RR)	0.11 (90% range 0.02–0.46)	0.27 (90% range 0.10–0.63)	0.31 (90% range 0.14–0.70)

Fund through the Met Office Climate Science for Service Partnership (CSSP) China as part of the Newton Fund, the EUCLEIA project funded by the European Union's Seventh Framework Programme [FP7/2007–13] under Grant Agreement No. 607085, and by the Joint U.K. DECCBEIS/Defra et Office Hadley Centre Climate Programme (GA01101).

REFERENCES

Allen, M., and P. Stott, 2003: Estimating signal amplitudes in optimal fingerprinting. Part I: Theory. *Climate Dyn*., **21**, 477–491, doi:10.1007/s00382-003-0313-9.

Cao, L., Y. Zhu, G. Tang, and Z. Yan, 2016: Climatic warming in China according to a homogenized data set from 2419 stations. *Int. J. Climatol*., **39**, 4384–4392, doi:10.1002/joc.4639.

CMA, 2017: *China Climate Bulletin 2016*. China Meteorological Administration, 50 pp.

Cohen, J., and Coauthors, 2014: Recent Arctic amplification and extreme mid-latitude weather. *Nat. Geosci*., **7**, 627–637, doi:10.1038/ngeo2234.

MOST (Ministry of Science and Technology), 2016: *Third National Assessment Report on Climate Change* (in Chinese). China Science Press, 976 pp.

Jiang, Q., X. K. Ma, and F. Wang, 2016: Analysis of the January 2016 atmospheric circulation and weather (in Chinese). *Meteor. Mon*., **42**, 514–520, doi:10.7519/j.issn.1000-0526.2016.04.16.

Lu, C., Y. Sun, H. Wan, X. B. Zhang, and H. Yin, 2016: Anthropogenic influence on the frequency of extreme temperatures in China. *Geophys. Res. Lett*., **43**, 6511–6518, doi:10.1002/2016GL069296.

Mori, M., M. Watanabe, H. Shiogama, J. Inoue, and M. Kimoto, 2014: Robust Arctic sea-ice influence on the frequent Eurasian cold winters in past decades. *Nat. Geosci*., **7**, 869–873, doi:10.1038/ngeo2277.

Ribes, A., S. Planton, and L. Terray, 2013: Application of regularised optimal fingerprinting to attribution. Part I: Method, properties and idealised analysis. *Climate Dyn*., **41**, 2817–2836, doi:10.1007/s00382-013-1735-7.

Santer, B. D., and Coauthors, 2014: Volcanic contribution to decadal changes in tropospheric temperature. *Nat. Geosci*., **2**, 185–189, doi:10.1038/ngeo2098.

Sun, Y., and Coauthors, 2014: Rapid increase in the risk of extreme summer heat in Eastern China. *Nat. Climate Change*, **4**, 1082–1085, doi:10.1038/nclimate2410.

Trenary, L., T. DelSole, M. K. Tippett, and B. Doty, 2016: Extreme eastern U.S. winter of 2015 not symptomatic of climate change [in "Explaining Extreme Events of 2015 from a Climate Perspective"]. *Bull. Amer. Meteor. Soc*., **97** (12), S31–S35, doi:10.1175/BAMS-D-16-0156.1.

Wolter, K., M. Hoerling, J. K. Eisheid, G. J. van Oldenborgh, X.-W. Quan, J. E. Walsh, T. N. Chase, and R. M. Dole, 2015: How unusual was the cold winter of 2013/14 in the upper Midwest? [in ''Explaining Extreme Events of 2014 from a Climate Perspective'']. *Bull. Amer. Meteor. Soc*., **96** (12), S10–S14, doi:10.1175/BAMS-D-15-00126.1.

Yin, H., Y. Sun, H. Wan, X. Zhang, and C. Lu, 2016: Detection of anthropogenic influence on the intensity of extreme temperatures in China. *Int. J. Climatol*., **37**, 1229–1237, doi:10.1002/joc.4771.